RESEARCH ARTICLE

Synthesis, Characterization of New Ligand Derived from 4-aminoantipyrine and its Complexes with Few Metallic Ions and Evaluation of their Activity as Anticancer

M. N. Dawood, H. O. Jamel

Department of Chemistry, College of Education, University of Al-Qadisiyah, Diwaniya, Iraq

Received: 21st October, 2022; Revised: 07th November, 2022; Accepted: 25th November, 2022; Available Online: 25th December, 2022

ABSTRACT

A new heterocyclic ligand (LH) derived from 4-aminoantipyrene was prepared through the reaction of 2-mercaptobenzothiazole with 4-amino-antipyrene dissolved in absolute ethanol as the first step to form compound-A, while the second step involved the reaction of *O*-phenylenediamine with benzil to produce compound -B, the third step involved the reaction of the products of the first and second steps to give the ligand as a final product. Five complexes, Ni (II), Cu (II), Zn(II), Cd (II) and Ag (I) were synthesized from the reaction of the ligand (LH) with its ionic salts. The ligand and its prepared complexes are characterized by proton nuclear magnetic resonance (^{1}H-NMR), fourier-transform infrared spectroscopy (FTIR), UV-vis spectroscopy and X-rays as well as used other techniques such as quantitative analysis of the elements china health and nutrition survey (CHNS), field emission scanning electron microscope (FESEM) as well as molar conductivity and magnetism sensitivity, in addition to measuring melting points. These techniques were used to determine the structures and geometry of the prepared compounds.

FTIR spectra showed that the ligand behaves as a tetra-dentate ligand and that the ratio of ligand to metal is (1:1) for all the prepared complexes according to the molar ratio calculations, which were confirmed by quantitative analysis of the elements CHNS and atomic absorption measurements. The molar conductivity results showed that all the non-electrolytic complexes except the zinc (II) and cadmium (II) complexes were ionic in a 1:1 ratio. From the foregoing, it is proved that the complexes have tetrahedral geometry, with the exception of the Ni(II) and Cu(II) complexes, which are octahedral. The anticancer activity of the ligand and its complex with silver was further evaluated using breast cancer cell lines and compared to the normal cell line. The study showed good results by treating infected cells compared to normal cells.

Keywords: Anticancer activity, Antipyrine, Benzothiazole ligands, Benzothiazole complexes, Schiff base-ligands.

International Journal of Drug Delivery Technology (2022); DOI: 10.25258/ijddt.12.4.32

How to cite this article: Dawood MN, Jamel HO. Synthesis, Characterization of New Ligand Derived from 4-aminoantipyrine and its Complexes with Few Metallic Ions and Evaluation of their Activity as Anticancer. International Journal of Drug Delivery Technology. 2022;12(4):1669-1681.

Source of support: Nil.

Conflict of interest: None

INTRODUCTION

Antipyrine is a heterocyclic compound with the molecular formula $C_{11}H_{12}N_2O$[1] and a derivative of 1,2-dihydropyrazol-3-one-pyrazolone, replaced by a methyl group at C-1 and C-5 and with a phenyl group at N-2.[2,3] It has a role as a non-narcotic analgesic, antipyretic, non-steroidal anti-inflammatory, cyclooxygenase inhibitor, antibiotic.[4,5] It is a white or crystalline, colorless and odorless powder that is soluble in distilled water and ethanol alcohol.[6] Antipyrine is a low-toxicity drug that was first prepared by Connor in 1883 AD.[7,8]

Benzothiazoles are bicyclic compounds that are heterocyclic organic compounds containing a benzene ring attached to a five-membered thiazole ring containing nitrogen and sulfur atoms.[9] It is a weak base and is a colorless and slightly viscous liquid with a melting point of (2°C), boiling point (227–228°C) and is slightly soluble in water.[10]

Benzothiazoles were first prepared by the scientist Hofmann in the year 1887 AD.[11] Benzothiazoles are of great importance nowadays, as benzothiazoles and their derivatives are found in synthesizing many compounds of great importance in biochemistry and medicine.[12,13] It is present in the chemical formula of most drugs used in the treatment of many diseases, as it is used as an anti-inflammatory and antimicrobial, including bacteria of all types. These compounds have also been used as an anti-fungal, anti-cancer, anthelmintic and anti-diabetic.[14,15]

Huggo schiff was the first to prepare schiff's bases in 1864,[16] through a condensation reaction between aldehydes

**Author for Correspondence: haider.hassani@qu.edu.iq*

or ketones with primary amines with the removal of water molecules.[17,18] Schiff bases are involved in many fields, whether scientific, industrial or agricultural.[19] They have been found to be of great importance in life processes, such as reactions involving the transfer of an amine group *via* a non-enzymatic transfer reaction of bacteria and fungi.[20]

Schiff bases are among the ligands used in coordination chemistry, as they enter into the preparation of many complexes with metallic elements, especially transition elements, due to their ability to coordinate and thus form complexes with different structures and various uses.[21,22]

In this study, a ligand schiff base-type derived from 4-aminoantipyrine and its metal complexes with Ni(II), Cu(II), Zn(II), Cd(II) and Ag(I) were synthesized. The effectiveness of the prepared ligand and its complex with silver (I) were evaluated as anti-cancer.

EXPERIMENTAL

Materials and Measurements

All chemicals and solvents of high purity are obtained from various companies such as Fluke, B.D.H, Merck, JT.Baker, Scharlu , Sigma and Aldrich.

The elemental analysis of the prepared ligand and its metallic complexes was carried out using a device micro analytical unit of EA 300 C.H.N Element analyzer (Shahid Beheshti University, Iran). Proton nuclear magnetic resonance (^{1}H-NMR) spectrum were recorded with a Bruker 500 MHZ spectrophotometer, dimethyl sulfoxide (DMSO) as a solvent and TMS as an internal standard (Shahid Beheshti University, Iran). Infrared spectra were recorded using KBr discs and using a shimadzu 8400S fourier-transform infrared spectroscopy (FTIR) at a range of (400–4000) cm^{-1}. The electronic spectra were measured using a shimadzu 1650 pc in absolute ethanol as a solvent and concentration (10^{-3}M) within the range (200–900) nm. The metal content of the complexes was measured using atomic absorption technique by shimadzu AA-6300. X-ray diffraction (XRD) were measured using Bestec Germany Aluminum anode model X pertpro, the wavelength of X-ray beam (Cu kα) 1.54 Aº, Anod material=Cu, the voltage = 40KV and current = 30 mA (Shahid Beheshti University, Iran). Field-emission scanning electron microscope (FESEM) images were taken using a device (TESCAN MIRA3, Czech) (Shahid Beheshti University, Iran). The magnetic susceptibility of the prepared complexes were measured at room temperature using the Faraday method; the magnetic correction was used and performed by Pascal's constants. These measurements were performed using (Balance Magnetic Susceptibility Model-M.S.B Auto).[23] Molar conductivity measurements were recorded at room temperature at a concentration (10^{-3} M) by using conductivity bridge model 31A. The melting points of the ligand and its complexes were measured by using electrothermal melting point 9300.

Synthesis of Ligand 2-((2-((-4-(benzo[d]thiazol-2-ylamino)-1,5-dimethyl-2-phenyl-1,2-dihydro-3H-pyrazol-3-ylidene)amino)phenyl)imino)-1,2-diphenylethan-1-ol (LH)

The ligand wea synthesized in three steps:

The First Step

The formation of compound (A) by taking 2.03 g of 4-aminoantipyrine and dissolving it in 25 mL of absolute ethanol, then weighing 1.67 g of mercaptobenzothizole and dissolving in 25 mL of ethanol, mixing the two solutions in a round about, the mixture refluxed for eight hours. Follow up the reaction with lead acetate paper, where the blackening of the paper stops, indicating the end of the reaction. The precipitate was collected, dried and recrystallized with hot ethanol, then dried (74%) and (87–89ºC).

The Second Step

The formation of compound (B), which includes a weight of 1.08 g of orthophenylene diamine and dissolving it in 25 mL of absolute ethanol and taking a weight of 2.12 g of benzoin and dissolving it in 25 mL of absolute ethanol with the addition of 4–5 drops of acetic acid after that, the two solutions are mixed in a circular flask, and the refluxed process begins for

Table 1: Some of physical properties of the ligand (LH) and its metal complexes

Compounds	*color*	*MP (°C)*	*Yield %*	*M. Wt.*	*Elemental analysis (%): Found (calcd.)*				
					C	*H*	*N*	*S*	*M*
Ligand (LH)	Light yellow	120–122	72	$C_{38}H_{32}N_6OS$ 620.78	73.52 (74.15)	5.20 (5.38)	13.54 (13.72)	5.16 (5.41)	--
[Ni(L) (H_2O)Cl]	Light brown	130–132	79	$C_{38}H_{33}Cl_2NiN_6O_2S$ 767.38	59.48 (60.23)	4.33 (4.79)	10.95 (11.27)	4.18 (4.52)	7.65 (8.22)
[Cu(L) (H_2O)Cl]	Light yellow	136–138	85	$C_{38}H_{33}Cl_2CuN_6O_2S$ 772.23	59.10 (59.65)	4.31 (4.69)	10.88 (11.51)	4.15 (4.38)	8.23 (8.58)
[Zn(L)] Cl	Brown	128–130	78	$C_{38}H_{31}ClZnN_6OS$ 720.60	63.34 (63.87)	4.34 (4.51)	11.66 (11.83)	4.45 (4.74)	9,07 (9.38)
[Ag (L)]	Light green	126–128	67	$C_{38}H_{31}AgN_7O_4S$ 789.64	57.80 (58.38)	3.96 (4.23)	12.42 (12.85)	4.06 (4.51)	13.66 (14.19)
[Cd(L)]Cl.H_2O	Light brown	188–190	74	$C_{38}H_{33}Cl_2CdN_6O_2S$ 821.10	55.59 (56.38)	4.05 (4.74)	10.24 (10.88)	3.90 (4.22)	13.69 (14.16)

eight hours, and the precipitate is collected after the end of reflux by filtering it, then drying it, then recrystallizing using hot ethanol and drying, giving a product (84%) and a melting point and (98–100°C).

The Third Step

Included the reaction of (3.36 g) of compound (A) dissolved in 25 mL of absolute ethanol with (3.02 g) of compound (B) dissolved in 25 mL of absolute ethanol, (4–5 drops) of glacial acetic acid were added to compound (A), mix the above two solutions, then reflux of the mixture for 8 hours, a precipitate was formed, filtered, then dried the product and recrystallized to give the ligand with the percentage (72%) and melting point (120–122°C).

Synthesis of Metallic Complexes

Ligand (LH) complexes were prepared according to the following general method:

A solution of 0.31 g dissolved in 10 mL of absolute ethanol from ligand (LH) was added to a solution of 0.5 mmol of transition metal chloride, except for silver, where silver nitrate was used in 10 mL of absolute ethanol, the mixture was refluxed with stirring for two hours and then cooled , where the formation of precipitates was observed that were filtered, dried and recrystallized in absolute ethanol, colored and pure precipitates were obtained from metal ion complexes whose physical properties are shown in Table 1.

RESULT AND DISCUSSION

Characterization of Ligand (LH) and its Metal Complexes

The ligand (LH) is characterized as light-yellow crystals, but the five complexes prepared from them change from the color of light brown, light yellow, light green, light yellow as well as light brown. The ligand and its prepared complexes are soluble in most organic solvents, such as ethanol, methanol, DMSO and DMF, but they are insoluble in distilled water.

Metal: Ligand Ratio

The [M:L] ratio of the complexes was determined by the molar ratio method at the maximum wavelength.

An equal concentration of each of the ligand (LH) and metal ion salts was prepared ($1x10^{-4}$ M), a fixed volume of the metal salt and increasing volumes of ligand(LH) solutions are taken, then the absorbance is measured for each solution at the maximum wavelength, the relationship between the absorbance and the molar ratio (V_L/V_M) is drawn, which results in two straight lines whose intersection point represents the ratio of the ligand to the metal [L:M], as the ratio was [1:1]. When comparing these percentages with the percentages obtained from the elemental analysis, it was found that they are similar.[24,25]

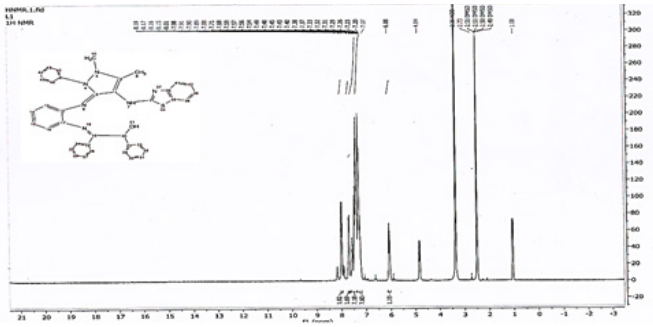

Figure 1 : The ^{1}H-NMR spectrum of the synthesized ligand (LH)

^{1}H-NMR Spectra

The ^{1}H-NMR spectrum of the ligand (LH) was studied using DMSO-d_6 as the solvent and TMS as the internal reference. The spectrum showed two single signals at (S, 3H , δ = 1.08 ppm) and (S, 3H, δ =2.73 ppm) belonging to the protons of the two methyl groups (C-CH_3 and N-CH_3), respectively,[26] while the signal at (S, H, δ = 4.84 ppm), which due to proton of methyne group (CH-OH) and signal at (S, H, δ = 6.08ppm) refer to hydroxyl group proton (Figure 1).[27]

Multiple other signals are observed in (M, 10H, δ= 7.07–7.37 ppm) related to the protons of the two phenyl rings of benzoin.[28] Also, several signals appeared at (M, 5H, δ= 7.38–7.48 ppm) related to the protons of phenyl ring of pyrazole.[29] The spectrum also gave multiple signals at (M, 4H, δ= 7.54–7.91 ppm) belonging to the protons of phenyl ring of *O*-phenylene di-amine.[30] While multiple signals appeared at (M, 4H, δ= 7.98–8.17 ppm) belonging to the phenyl ring protons belonging to benzothiazole ring,[31] while the single signals at (S, 1H, δ = 8.18 ppm) indicate to the proton of a secondary amine group proton.[32]

Table 2: The important infrared spectral bands of ligand (LH) and its prepared complexes

Compounds	υ*(O-H) (H_2O)*	υ*(O-H) Benzoin*	υ*(N-H) 2°amine*	υ*(C=N) Imine*	υ*(C=N) Benzothiazole ring*	υ*(M–N)* υ*(M–O)*
Ligand (LH)	-	3409	3379	1681	1596	—
[Ni(L) (H_2O)Cl]	3453	-	3342	1662	1596	509 455
[Cu(L) (H_2O)Cl]	3458	-	3365	1668	1596	516 424
[Zn(L)] Cl	-	-	3323	1664	1596	501 463
[Ag (L)]	-	-	3346	1653	1596	558 436
[Cd(L)]Cl.H_2O	3442	-	3306	1665	1596	563 462

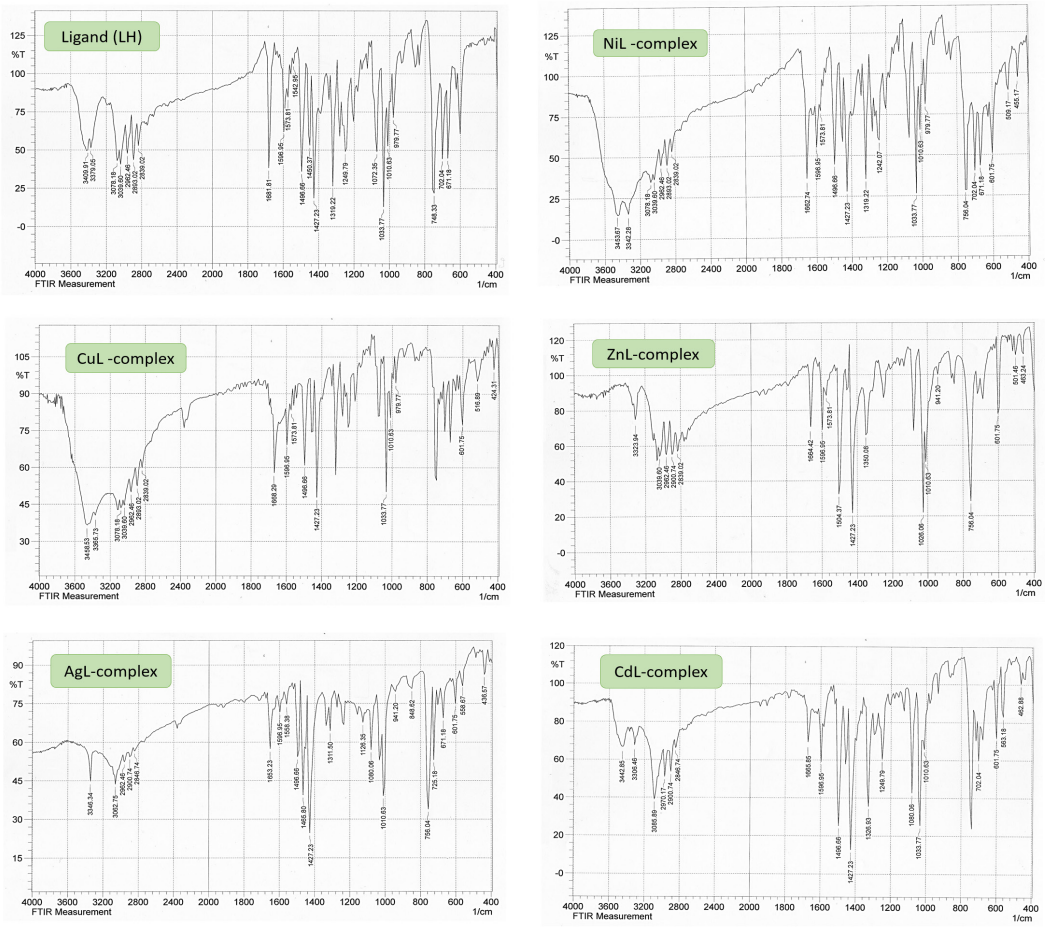

Figure 2: The FTIR spectra of the ligand (LH) and its metallic complexes.

Infrared Spectra of the Ligand (LH) and its Metal Complexes

Infrared spectra were measured using Shimadzu 8400S device and using potassium bromide (KBr), infrared spectra were used to identify the functional groups in the ligand and their complexes. The spectrum of the free ligand showed two clear bands at (3409 and 3379 cm^{-1}), which belong to the hydroxyl υ(OH) and secondary amine groups υ(NH), respectively.[33] A band appeared in the spectrum of the ligand at (1681 cm^{-1}), an important band whose appearance indicates the formation of the ligand, which is the azomethine group (C = N) that belongs to the schiff base,[34] while the carbonyl group band in the reactants before the reaction disappears. Other bands appeared in (3078 cm^{-1}) and (2962 and 2893 cm^{-1}), which belong to the (C-H) aromatic and aliphatic groups, respectively,[35] as for the groups (C=C) aromatic, it gave bands at (1496, 1573 cm^{-1}), finally, other bands exhibited at (1596, 1010 cm^{-1}) due to the functional groups υ (C = N) and (C-S) of the benzothiazole ring, respectively (Figure 2).[36]

From observing the spectra of the prepared complexes and comparing it with the spectrum of the free ligand, it was found:

The azomethine group υ (C=N) belonging to the schiff base was shifted towards lower frequencies compared to what it was in the spectrum of the free ligand and appeared at (1662, 1668, 1664, 1653 and 1665 cm^{-1}) in the spectra of the prepared complexes,[37] the frequency of the secondary amine group (N-H), which appeared at (3379 cm^{-1}) in the spectrum of the ligand before coordination, was shifted to a lower frequency and appeared at the range (3306–3365 cm^{-1}) in the spectra of the prepared ligand (LH) complexes, the occurrence of this shift is strong evidence of the coordination of the ligand with the metal ions through the nitrogen atoms of the azomethine group and the secondary amine.[38]

The hydroxyl group of the free ligand disappeared in the spectra of the complexes due to the loss of its proton after coordination, which is another evidence of coordination and appearance bands at (424–463 cm^{-1}) , which indicated to υ (M-O). New broad bands also appeared at (3453, 3458 and 3442 cm^{-1}) belonging to the hydroxyl group of the hydrate water in the nickel(II), copper(II) and cadmium(II) complexes, respectively,[39] while the bands found at (501–563 cm^{-1}) mainly due to (M-N) groups (Tbale 2).[40]

Electronic Spectra and Magnetic Susceptibility Measurements

Metal complexes are considered colored compounds, and these colors vary from one complex to another according to the metal

Table 3: The electronic spectra, magnetic moment, and expected geometry of the ligand (LH) and its complexes

Compounds	*(nm)*	*υ^- (cm^{-1})*	*Transitions*	*μeff (B.M)*	*Geometry*
Ligand (LH)	207 258 322	48309 38760 31056	π-π* π-π* n-π*	——	——
[Ni(L) (H_2O)Cl]	220 293 352 463 616 746	45455 34130 28409 21598 16234 13405	Ligand Field Ligand Field Ligand Field ^3A_2g (F) $\rightarrow ^3T_1g$ (p) ^3A_2g (F) $\rightarrow ^3T1g$(F) ^3A_2g (F) $\rightarrow ^3T_2g$(F)	2.83	Octahedral sp^3d^2 regular
[Cu(L) (H_2O)Cl]	226 299 346 586	44248 33445 28902 17065	Ligand Field Ligand Field Ligand Field $^2B_1g \rightarrow ^2Eg$	1.75	Octahedral sp^3d^2 distorted
[Zn(L)] Cl	221 291 340	45249 34364 29412	Ligand Field Ligand Field Charge transfer(MLCT)	(Dia.)	Tetrahedral sp^3
[Ag (L)]	233 294 381	42918 34014 26247	Ligand Field Ligand Field Charge transfer(MLCT)	(Dia.)	Tetrahedral sp^3
[Cd(L)]Cl.H_2O	223 305 362	44843 32787 27624	Ligand Field Ligand Field Charge transfer(MLCT)	(Dia.)	Tetrahedral sp^3

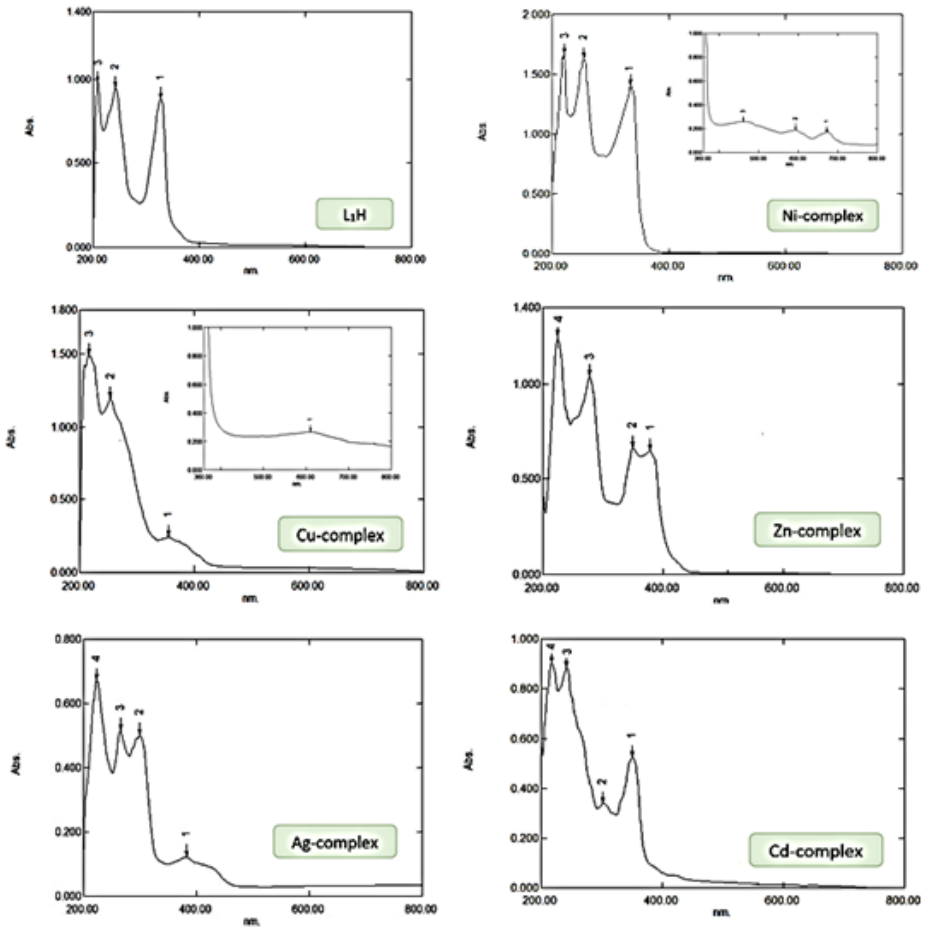

Figure 3: Electronic spectra of the ligand (LH) and its metallic complexes

present in the complex and from one ligand to another. The range of colors is an important evidence to the occurrence of coordination. The difference in color shows different absorption bands in intensity and position, which is another evidence of coordination. In order to more accurately identify the types of electronic transitions of ligands and their complexes, we must know the most important types of electronic transitions that occur in ligands and their complexes.

When observing the electronic spectrum of the ligand (LH), Figure 3, showed three absorption peaks at 207 (48309), 258 (38760) and 322 nm (31056 cm^{-1}), the first two peaks indicate to (π-π*) transmission of the azomethane (C = N) group (Table 3 and Figure 3).[41]

The Electronic Spectra of the Complexes

Nickel(II) Complex

By studying the spectrum of a nickel(II) complex, it was observed that the absorption peaks appeared at 220 (45455), 293 (34130) and 352 nm (28409 cm^{-1}), all of which refer to the spectrum of the ligand field, while the absorption peaks at 463 (21598), 616 (16234) and 746 nm (13405 cm^{-1}), which refer to the transitions ^3A_2g (F) $\rightarrow ^3T_1g$ (p), ^3A_2g (F) $\rightarrow ^3T1g$(F) and ^3A_2g (F) $\rightarrow ^3T_2g$(F), which showed that the complex is a regular octahedron (hyperdilation: sp^3d^2), the magnetic moment of this complex is (2.83 B.M), Which indicates the presence of two non-pair electrons.[42]

Copper(II)–Complex

The spectrum of the copper complex, showed several absorption peaks centered at 226 (44248), 299 (33445), 346 nm (28902 cm^{-1}), all of which belong to the spectrum of the ligand field, either Broad absorption at 586 nm (17065 cm^{-1}), due to $^2B_1g \rightarrow ^2Eg$, a wide band appeared due to the Jan-Teller distortion, giving the complex a distorted octahedral geometry (hyperdilation: sp^3d^2), the magnetic moment of copper (II) complex is (175 B.M), which indicates the presence of one non-pair electron in the (eg) level.[43]

Zinc(II), Silver(I) and Cadmium(II) Complexes

We note in the electronic spectra of each of the complexes of zinc(II) , silver(I), and cadmium(II) complexes that there are no (d-d) transitions in their spectra due to the saturation of the (d) orbitals by electrons, so their electronic spectra cannot be used to determine the structure and geometry of these complexes, the above complexes showed a number of peaks within the range 221–305 nm (45249–32787 cm^{-1}) which belong to the ligand field, while the peaks at 340, 381, 362 nm (29412, 26247, 27624 cm^{-1}), all refer to the charge transitions of the type (M → L) in zinc (II), silver (I) and cadmium (II)

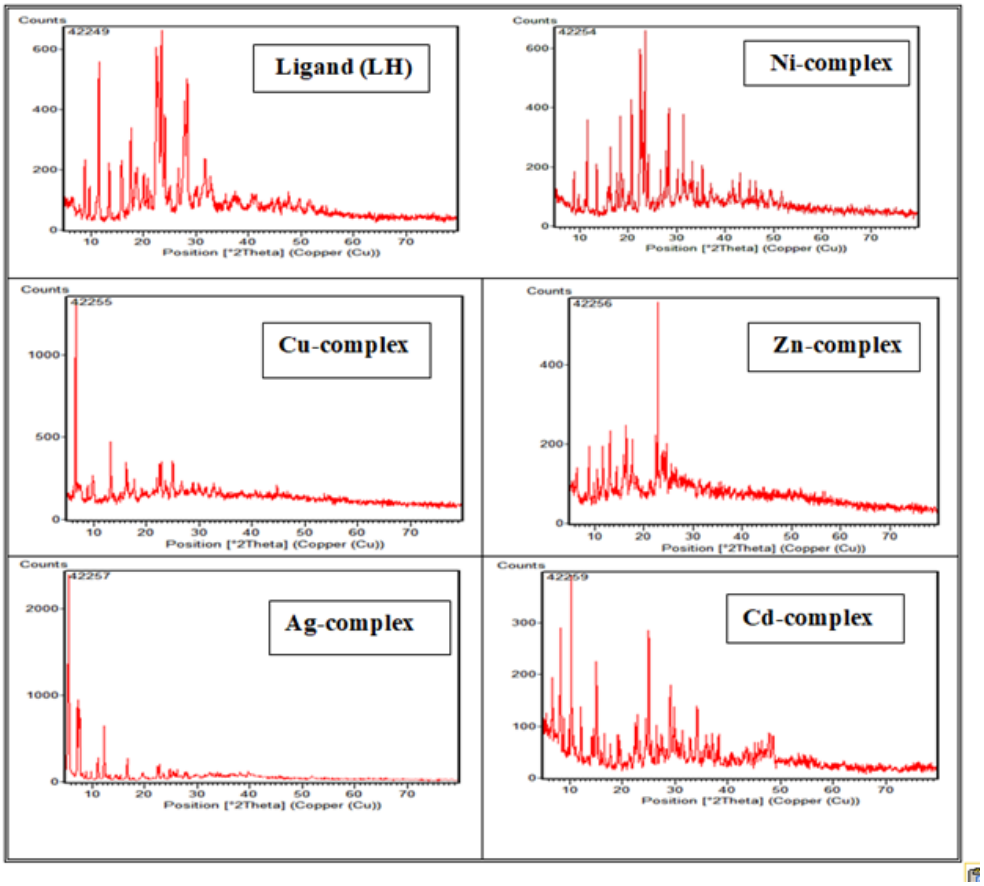

Figure 4: XRD patterns of Ligand (LH) and its complexes

Table 4: X-RD data of the ligand (LH) and metal complexes

Compound	*No.*	*°2Θ observed*	*d observed (A°)*	*I/I° (%)*	*FWHM*	*Crystallite Size. (nm)*	*Lattice Strain*
Ligand (LH)	1	11.574	7.639	96.7	0.187	44.62	0.0081
	2	22.814	3.894	71.2	0.710	11.93	0.0154
	3	22.828	3.892	69.4	0.710	11.93	0.0153
	4	23.498	3.782	100	0.517	16.4	0.0108
	5	28.346	3.146	71.5	0.546	15.680	0.0094
[Ni(L) (H_2O)Cl]]	1	11.613	7.613	57.2	0.135	15.95	0.0234
	2	18.417	4.813	55.4	0.126	66.74	0.0034
	3	20.705	4.286	66.6	0.142	59.429	0.0034
	4	23.524	3.778	100	0.492	17.23	0.0103
	5	28.390	3.141	58.8	0.151	56.71	0.0026
[Cu(L) (H_2O)Cl]	1	6.622	13.337	100	0.110	75.59	0.0083
	2	13.269	6.667	27.8	0.137	61	0.0051
	3	16.200	5.466	17.9	0.207	40.510	0.0063
[Zn(L)] Cl	1	13.156	6.724	33	0.0994	41.989	0.0075
	2	16.445	5.385	36	0.2092	20.07	0.0126
	3	22.526	3.943	30.8	0.0334	126.33	0.0015
	4	22.865	3.886	100	0.0334	126.41	0.0014
[Ag (L)]	1	5.570	15.854	100	0.220	37.78	0.0197
	2	7.526	11.736	34.3	0.352	23.630	0.0234
	3	11.170	7.915	11.4	0.212	39.339	0.0095
	4	12.326	7.174	27.9	0.123	67.88	0.0050
[Cd(L)]Cl.H_2O	1	8.296	10.648	72.6	0.108	77.07	0.0065
	2	10.316	8.568	100	0.155	53.779	0.0075
	3	15.096	5.864	55.5	0.151	55.46	0.005
	4	24.993	3.560	67.6	0.170	50.019	0.0033
	5	29.163	3.059	38.6	0.151	56.81	0.0025

complexes, respectively. Previous studies have shown that these complexes have regular tetrahedral geometry these complexes have diamagnetic properties.[44]

X-ray Diffraction Study (XRD)

The crystal structures of the ligand (LH) and its metal complexes under study were studied in their solid-state using X-ray diffraction within (angular range) 5–80°(2Θ) to know some structural properties such as crystal structure and crystal size. Macrostrains and dislocation density were also calculated in order to estimate the extent of its purity and the defects in the crystal structure when converting ligand to metal complexes. There are some diffraction peaks that appear as broad peaks for several reasons, including micro-strains such as lattice deformation, faulting due to crystal deformations, domain size of the crystal and distribution of domain size. The XRD spectrum showed the presence of sharp peaks for ligands and metal complexes, which indicates that they form a crystal lattice and others contain broad peaks indicative of non-crystalline structures amorphous structure and the sharpness of the peaks depends on the crystal arrangement and properties of the crystal lattice as well as on the crystal levels.[45,46]

The Debye-Scherer equation was used to calculate the crystal size of ligand (LH) and its metal complexes, as follows:

$$D = \frac{k\lambda}{\beta \cos\theta}$$

D :crystal size rate

k : shape factor which is usually about 0.9

λ : wavelength of X-rays, value CuKα = 1.54056 A°

β : total width half the maximum height FWHM

Θ : is the angle of deviation

as well as the following equation was used to calculate the micro-compliance

S = β cosθ/4

S : micro-compliance (Macrostrains)

β : the total width of half the maximum height

Θ : the angle of deflection

The following equation was used to calculate the decay density :

$$\delta = 1/D2$$

By analyzing the X-ray spectra showing the clear difference in the data mentioned previously, the crystal size, the microplasticity, the density of the dissolutions, as well as the

Ni-complex

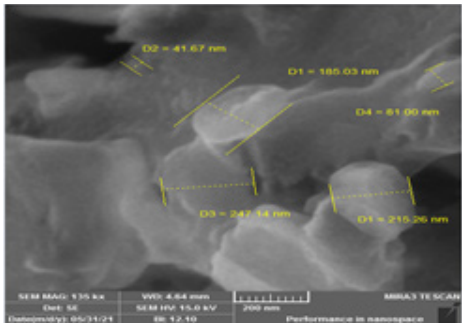

L_1H

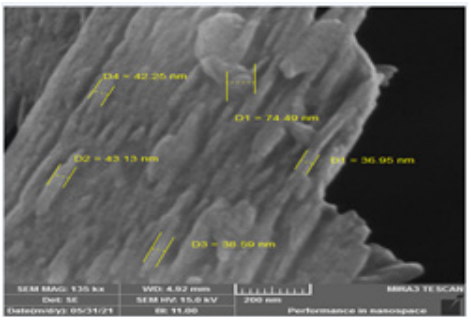

Ag-complex

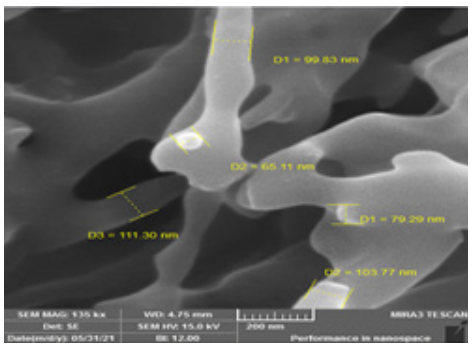

Cu-complex

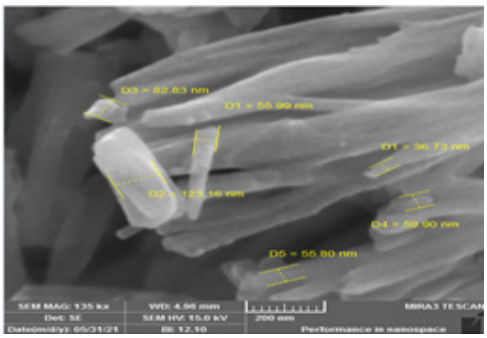

Cd-complex

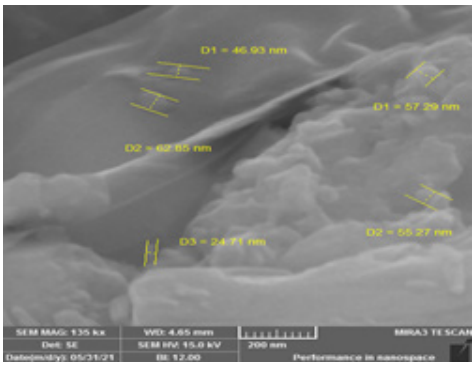

Zn-complex

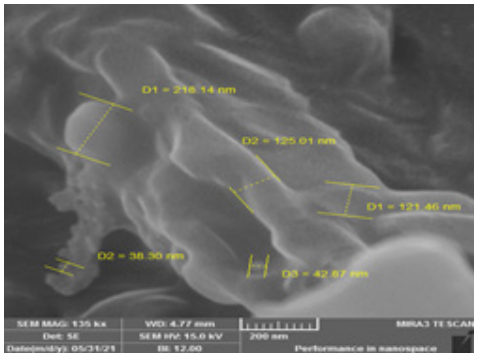

Figure 6: FE-SEM images of LH and its its complexes.

spacing between the crystal levels of ligand and its prepared metal complexes under study, and this confirms the occurrence of the coordination process between the ligand and the metal ions (Table 4).[47,48]

Emission Field Scanning Electron Microscopy Analysis (FESEM)

The scanning electron microscope technique was used to study the surface properties of ligand particles and its metal complexes with metallic ions of nickel(II), copper(II), zinc(II), silver(I) and cadmium(II), in terms of particle size and the clusters among them, depending on the cross-sectional distance is 200 nm and magnification strength Mag=135kx.

The FESEM analysis image of the ligand (LH) shows that it has the form of homogeneous and adjacent crystals and columns with an average particle size of 47.08 nm, while the FESEM analysis image of the nickel(II) complex appeared in the form of large, irregular crystals, with an average particle size of 154.02 nm, observed by analyzing the FESEM image of the Cu(II) complex, the particles are in the shape of adjacent columns, the average size of the particles is 69.06 nm, whereas, the FESEM image of the zinc (II) complex appeared as homogeneous spherical crystal particles with an average particle size of 168.64 nm, as for the FESEM image of the silver(I) complex, the particles appeared in the form of heterogeneous columns with an average particle size of 91.86 nm, also, the FESEM image of the cadmium(II) complex appeared in the form of heterogeneous crystal clusters and an average particle size of 49.41 nm.[49]

Through the FESEM images shown in the Figure 4 below, it was found that ligand (LH) and its metal complexes have a smaller grain size From 100 nm, that is, they are within the nanoscale, and some of the metal complexes are of a size higher than 100 nm, so they are outside the nanoscale range, and that the presence of some of the clusters is due to the agglomeration process, which leads to the assembly of primary particles, and the difficulty of getting rid of this phenomenon due to the use of temperatures High in order to complete the process of growing crystals of ligands and complexes, thus increasing the effective surface area, so it enters the quantitative effect to create new energy levels that lead to the free movement of the electron (Figure 5).[50]

Table 5: The effect of the ligand (LH) on the cells of MCF-7 and HEK-293e of the same concentration using MTT test for 24 hours.

Concentration (µg/mL)	*LH*					
	Cancer line cells MCF-7			*Normal line cells HEK-293*		
	Cell Viability		*% Cell Inhibition*	*Cell Viability*		*% Cell Inhibition*
	Mean	*SD*		*Mean*	*SD*	
16	94.89371	11.75687	5.10629	99.23274	2.68724	0.76726
31	88.32847	5.47589	11.67153	97.57033	6.25997	2.42967
62	59.62901	7.14765	40.37099	94.75703	9.45634	5.24297
125	27.44894	7.52134	72.55106	83.63117	6.13810	16.36829
250	6.83618	2.47927	93.16382	62.40409	7.20846	37.59591
500	6.17549	2.46799	93.82451	32.22506	7.39126	67.77494
IC_{50}	41.5			332		

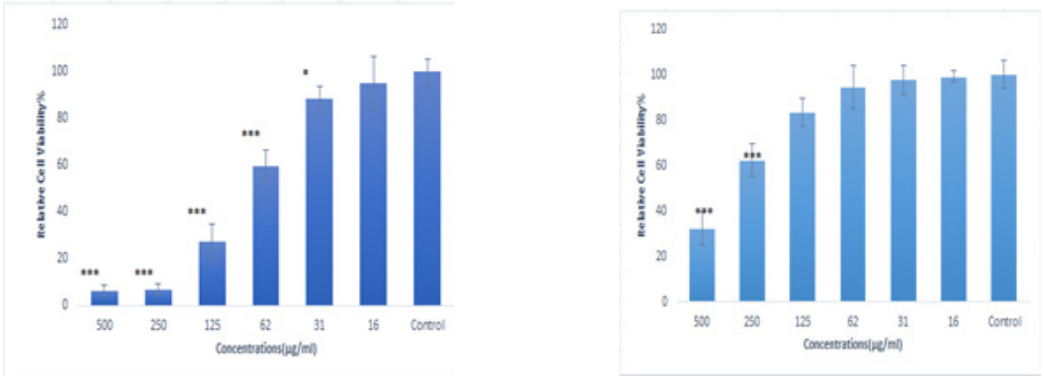

Figure 6: Comparison at viability and inhibition for the ligand in cancer and normal cells.

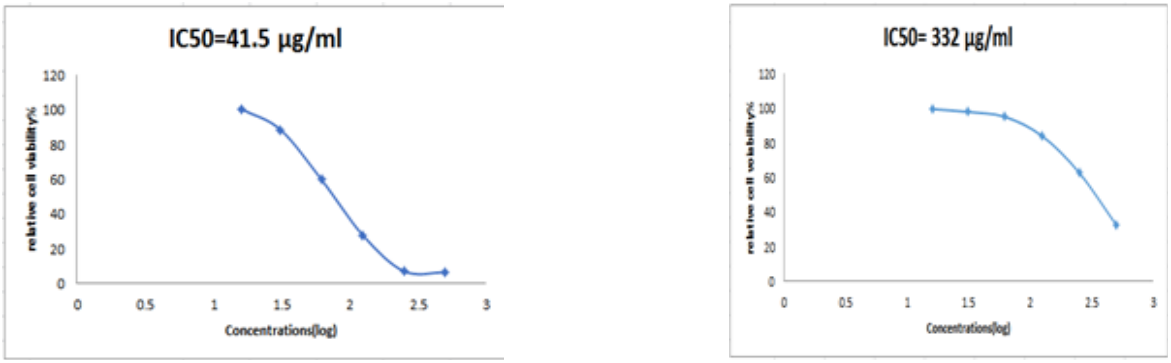

Figure 7: IC_{50} (µg/mL) values for the Ligand (LH) in MCF-7 cell line and normal cell line.

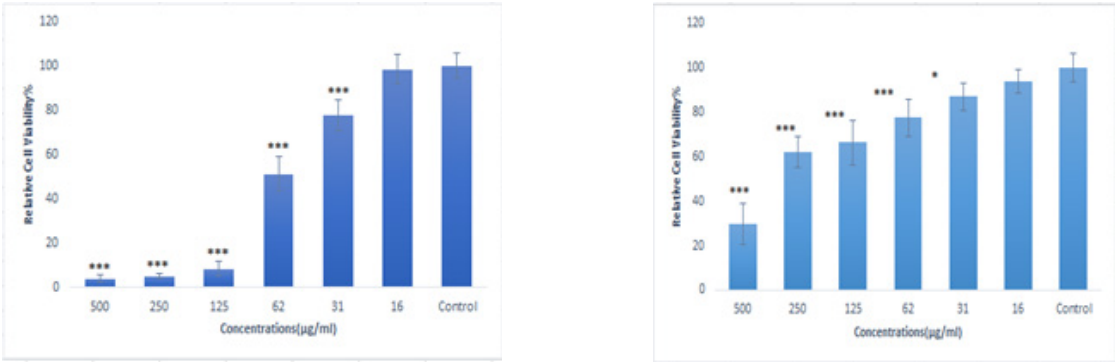

Figure 8: Comparison at viability and inhibition for the Ag (I) complex in cancer and normal cells

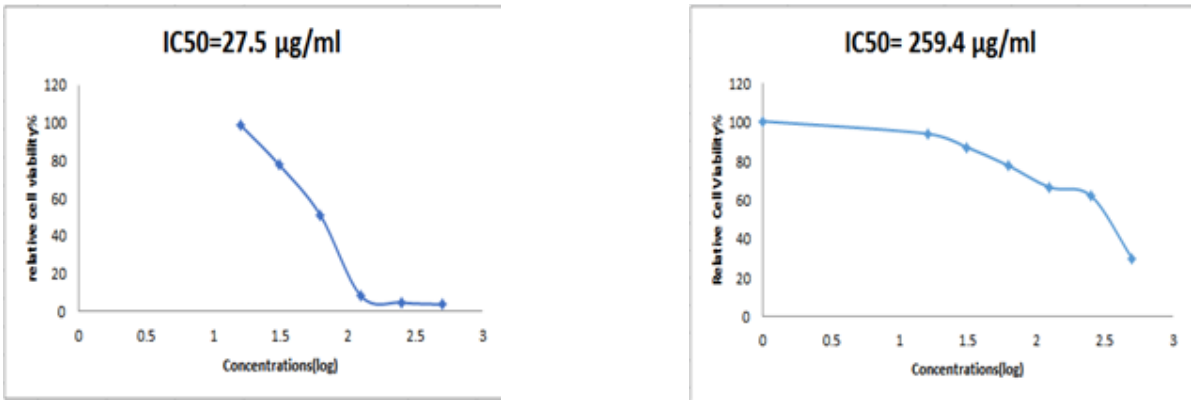

Figure 9: IC_{50} (µg/mL) values for the Ag(I) complex in MCF-7cell line and normal cell line

Table 6: The effect of the Ag (I) complex on the cells of MCF-7 and HEK-293 of the same concentration using MTT test for 24 hours.

Concentration (µg/mL)	*LHAg*					
	Cancer line cells MCF-7			*Normal line cells HEK-293*		
	Cell viability		*%Cell inhibition*	*Cell viability*		*%Cell inhibition*
	Mean	*SD*		*Mean*	*SD*	
16	98.64527	6.69719	1.35473	93.80252	5.39838	6.19748
31	77.56774	7.162944	22.43226	86.86975	6.11593	13.13025
62	51.31305	7.87318	48.68695	77.52101	8.33268	22.47899
125	8.274281	3.13919	91.72572	66.28151	9.94454	33.71849
250	4.77282	1.14452	95.22718	61.97479	6.946129	38.02521
500	3.83493	1.57915	96.16507	29.83193	9.22553	70.16807
IC_{50}	27.5			259.4		

Molar Conductivity Measurement

Molar conductivity measurements were used to determine whether the prepared compounds had ionic or non-ionic properties, where it was observed that the molar conductivity is directly proportional to the charged species in the solution, many organic solvents such as methyl cyanide, nitromethane, DMSO, DMF, ethanol and others are often used because they have a high dielectric constant and low viscosity.[51]

The molar conductivity of the ligand (LH) complexes were measured using absolute ethanol as a solvent at a concentration of ($1*10^{-3}$M) and at laboratory temperature. It was noticed that the zinc(II) and cadmium(II) complexes had conductivity values (36.3 and 36.8 $ohm^{-1}cm^2mole^{-1}$), respectively. These values indicate that these complexes have an ionic character in a ratio of (1:1), while the nickel(II) and copper(II) and silver(I) showed a relatively low conductivity (11.5, 9.5 and 8.5 $ohm^{-1}cm^2mole^{-1}$), these values indicated that they are complexes with non-ionic properties.[52]

Cytotoxicity by use Assays (MTT)

In this study, two types of cell lines were used, the breast cancer cell line MCF-7 and the healthy cell line HEK-293 for the purpose of comparison and showing their effectiveness on human cells and the possibility of using them as cancer drugs. The MTT test was used for bioassay of all cells. The results showed that the concentration of the prepared ligand (LH) and its complexes are of great importance in determining the percentage of cytostatic, and this phenomenon is called dose-dependent. When studying the effect of the ligand (LH) on the growth process of breast cancer cell lines (MCF-7) and normal healthy cells (HEK-293), it was observed that the least inhibition of the growth of breast cancer cells (MCF-7) and normal cells (HEK-293) at a concentration of 16 µg/mL, while the highest percentage of cytostatic was at a concentration of 500 µg/mL for cells of both lines.Where it was found that the percentage of the number of the remaining live cells after the reaction with the ligand ranged between (6.17549–94.89371%) for the cells of MCF-7, while the percentage of the remaining live cells of the (HEK-293) was between (32.22506–99.23274%). The best percentage of inhibition of the (MCF-7) at a concentration of 500 µg/mL was 93.824%, while the percentage of inhibition of the (HEK-293) at the same concentration was 67.774%.As for the (IC_{50}) in the case of the reaction of the ligand with the breast cancer cell line MCF-7, it was 41.5 µg/mL, while (IC_{50}) for normal cells HEK-293 was 332 µg/mL (Table 5 and Figure 6, 7).[53,54]

IC_{50} (µg/mL) values for the Ag(I) complex in MCF-7cell line and normal cell line. The effect of the silver(I) complex was studied on the growth process of (MCF-7) and (HEK-293). - (HEK-293) at a concentration of 16 µg/mL, while the highest percentage of cytostatics was at a concentration of 500 µg/mL for breast cancer cells (MCF-7) and healthy cells (HEK-293).

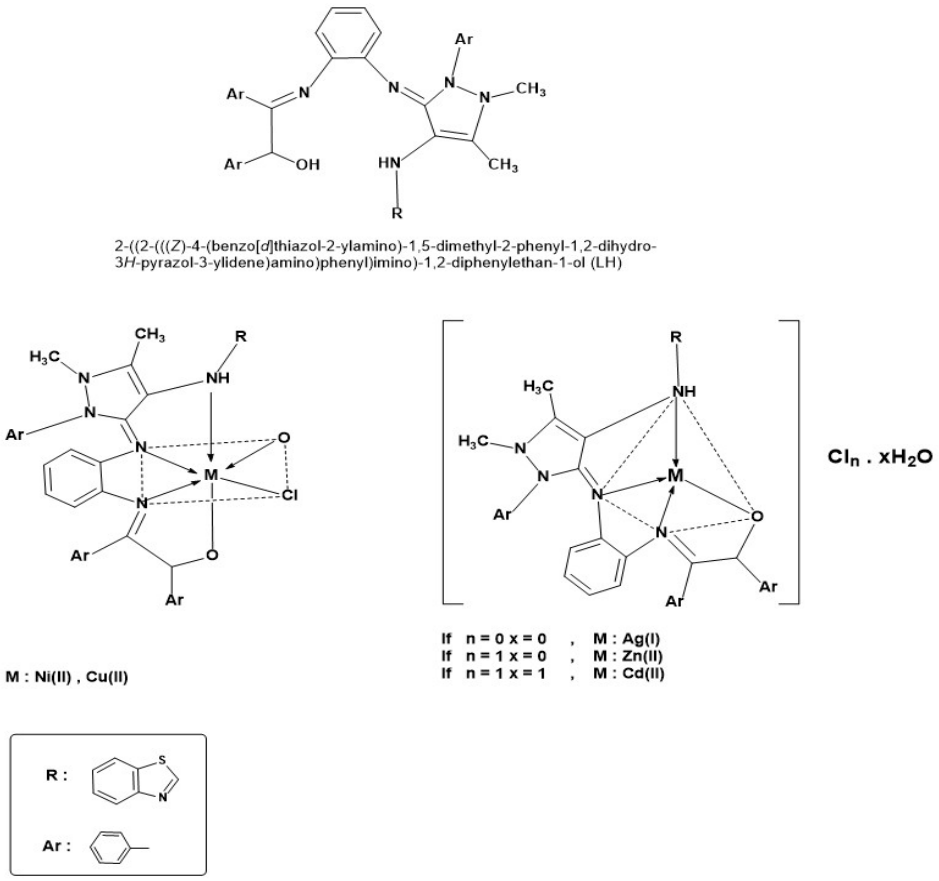

Figure 10: Proposed chemical structures of the ligand (LH) and its complexes

It was noted that the percentage of the number of live cells remaining after the reaction with the silver complex ranged between (3.83493–98.64527%) for the cells of MCF-7, while for cells of (HEK-293) was between (29.83193–93.80252%). The best percentage of inhibition of the breast cancer cell line (MCF-7) at a concentration of 500 µg/mL was 96.165069%, while the percentage of inhibition of the cell line of healthy cells (HEK-293) at the same concentration was 70.16807%. The half inhibitory concentration (IC_{50}) in the case of interaction of the silver complex with the cell line of MCF-7 was 27.5 µg/mL, while for normal cells HEK-293 was 259.4 (Table 6 and Figure 8-10).[55]

CONCLUSIONS

Spectroscopic methods (nuclear magnetic resonance, infrared and electronic spectra), in addition to X-ray diffraction, FESEM, molar conductivity, atomic absorption, microanalysis measurements of the elements, and melting points were used to determine the chemical structures of ligand(LH) and its prepared complexes. From the results of the above techniques, it was found that the geometry of the tetrahedral for all complexes, with the exception of the nickel(II) and copper(II) complexes, are octahedral, the ligand (LH) behaves as a tetradentate ligand. Anticancer tests showed that ligand (LH) and its complex with a silver(I) have good efficacy in reducing the growth of cancer cells.

REFERENCES

1. BAYTAŞ S, Inceler N, Mavaneh KF, ULUDAĞ MO, ABACIOĞLU N, GÖKÇE M. Synthesis of antipyrine/pyridazinone hybrids and investigation of their in vivo analgesic and anti-inflammatory activities. Turkish Journal of Chemistry. 2012;36(5):734-48.
2. Abu-Melha S. Synthesis, modeling study and antioxidants activity of new heterocycles derived from 4-antipyrinyl-2-chloroacetamidothiazoles. Applied Sciences. 2018 Nov 2;8(11):2128.
3. Ei Ashry ES, Awad LF, Ibrahim EI, Bdeewy OK. Synthesis of antipyrine derivatives derived from dimedone. Chinese Journal of Chemistry. 2007 Apr;25(4):570-3.
4. Demirci S. Synthesis and biological activity studies of some new hybrid compounds derived from antipyrine. Heterocyclic Communications. 2016 Jun 1;22(3):143-9.
5. Bedeui ZM. Synthesis And Characterization Of Schiff-Base Ligand Derivative From 4-Aminoantipyrine And Its Transition Metal Complexes. مجلة الكوفة للكيمياء| Kufa Journal for Chemistry. 2013 Dec 21;1(8).
6. Mohanram I, Meshram J. Synthesis and biological activities of 4-aminoantipyrine derivatives derived from betti-type reaction. International Scholarly Research Notices. 2014;2014.
7. Saeed A, Khurshid A, Flörke U, Echeverría GA, Piro OE, Gil DM, Rocha M, Frontera A, El-Seedi HR, Mumtaz A, Erben MF. Intermolecular interactions in antipyrine-like derivatives 2-halo-N-(1, 5-dimethyl-3-oxo-2-phenyl-2, 3-dihydro-1 H-pyrazol-4-yl)

benzamides: X-ray structure, Hirshfeld surface analysis and DFT calculations. New Journal of Chemistry. 2020;44(45):19541-54.
8. Aljamali NM, Aati SA, Obaid NH, Wannas FA. A Literature Review on Antipyrinein Chemistry Fields. American International Journal of Sciences and Engineering Research. 2019 Jan 24;2(1):9-21.
9. Keri RS, Patil MR, Patil SA, Budagumpi S. A comprehensive review in current developments of benzothiazole-based molecules in medicinal chemistry. European Journal of Medicinal Chemistry. 2015 Jan 7;89:207-51.
10. Srivastava A, Mishra AP, Chandra S, Bajpai A. Benzothiazole derivative: A review on its pharmacological importance towards synthesis of lead. Int. J. Pharm. Sci. Res. 2019;10(4):1553-66.
11. Le Bozec L, Moody CJ. Naturally occurring nitrogen–sulfur compounds. The benzothiazole alkaloids. Australian journal of chemistry. 2009 Jul 13;62(7):639-47.
12. Khokra SL, Arora K, Mehta H, Aggarwal A, Yadav M. Common methods to synthesize benzothiazole derivatives and their medicinal significance. International Journal of Pharmaceutical Sciences and Research. 2011;2(6):1356-78..
13. AL-Khazraji SI. Synthesis and characterization of some heterocyclic compounds derived from 2-mercapto benzothiazole. InAIP Conference Proceedings 2020 Dec 4 (Vol. 2290, No. 1, p. 030013). AIP Publishing LLC.
14. Shanthalakshmi K, Mahesh B, Belagali S. Synthesis of Benzothiazole Schiff's Bases and screening for the Antioxidant Activity. J. Chem. Pharm. Res. 2016 Dec 25;8(10):240-3.
15. Mahmood ZM, Ahmad AK. Synthesis of Some Heterocyclic Compounds Derived From 2-Amino Benzothiazole. JOURNAL OF EDUCATION AND SCIENCE. 2020 Dec 1;29(4):193-205.
16. Shah SS, Shah D, Khan I, Ahmad S, Ali U, Rahman AU. Synthesis and antioxidant activities of Schiff bases and their complexes: An updated review. Res. Appl. Chem. 2020;10:6936-63.
17. Kajal A, Bala S, Kamboj S, Sharma N, Saini V. Schiff bases: a versatile pharmacophore. Journal of Catalysts. 2013 Aug 27;2013.
18. Kareem IK, Hadi MA. Synthesis and Characterization Of Some transition Metal Complexes with New Azo-Schiff base ligand 3, 4-bis (((1E, 2E)-2-((2-((4-((Z)-(3-hydroxyphenyl) diazenyl) naphthalen-1-yl) amino) ethyl) imino)-1, 2-diphenylethylidene) amino) phenyl)(phenyl) methanone. Egyptian Journal of Chemistry. 2020 Jan 1;63(1):301-13.
19. Al Zoubi W, Al-Hamdani AA, Ahmed SD, Ko YG. A new azo-Schiff base: Synthesis, characterization, biological activity and theoretical studies of its complexes. Applied Organometallic Chemistry. 2018 Jan;32(1):e3895.
20. KAREEM EK, DREA AA, LATEEF SM. Investigation study of transition state for synthesis new schiff base ligands of isatin derivatives. Int. J. Chem. Sci. 2016;14(2):513-28.
21. Kareem IK, Waddai FY, Abbas GJ. Synthesis, Characterization and biological activity of Some Transition Metal Complexes with New Schiff Base Ligand Type (NNO) Derivative from Benzoin. Journal of Pharmaceutical Sciences and Research. 2019;11(1):119-24.
22. Ibatte SN. Synthesis and Characterization of N2O2 type Metal Complexes derived from 4-Aminoantipyrine, 4-Nitrobenzaldyhyde and Acetylacetone. Asian Journal of Research in Chemistry. 2017 Apr 28;10(2):166-73.
23. Speidel KH, Kenn O, Nowacki F. Magnetic moments and nuclear structure. Progress in Particle and Nuclear Physics. 2002 Jan 1;49(1):91-154.
24. Al-Adilee KJ, Alshamsi HA, Dawood MN. Synthesis, Spectral Characterization and photo Thermal Decomposition Studies of New Hetrocyclic Azo Dye Compound Derived From Imidazole with Some Transition Metal Complexes. Research Journal of Pharmaceutical, Biological and Chemical Sciences. 2016 Jul 1;7:2882-905.
25. Wear JO. Mathematics of The Variation and Mole Ratio Methods of Complex Determination. Journal of the Arkansas Academy of Science. 1968;22(1):97-101.
26. Maddila S, Gorle S, Seshadri N, Lavanya P, Jonnalagadda SB. Synthesis, antibacterial and antifungal activity of novel benzothiazole pyrimidine derivatives. Arabian Journal of Chemistry. 2016 Sep 1;9(5):681-7.
27. Alhaidry WA, Jamel HO. Synthesis and characterization of new benzothiazole-derived ligand and its complexes with some transitional metal ions with evaluation of their biological activities. Journal of Pharmaceutical Sciences and Research. 2018 Dec 1;10(12):3241..
28. Al-Bayati YK. Preparation of Selective Sensors for Cyproheptadine Hydrochloride based on Molecularly Imprinted Polymer used N, N-Diethylaminoethyl Methacrylate as Functional Monomer. Eurasian Journal of Analytical Chemistry. 2018;13:5.
29. Salman SR, Jamel HO. Preparation, Characterization and Evaluation of the Biological Activity of the New Ligand Derived from 2-Mercaptobenzimidazole, a Type of Schiff Bases and its Complexes with some Metal Ions. Solid State Technology. 2020 Jul 30;63(1):1612-26.
30. Kyhoiesh HA, Al-Adilee KJ. Synthesis, spectral characterization and biological activities of Ag (I), Pt (IV) and Au (III) complexes with novel azo dye ligand (N, N, O) derived from 2-amino-6-methoxy benzothiazole. Chemical Papers. 2022 May;76(5):2777-810.
31. Sedaghat N, Naimi-Jamal M, Mokhtari J. Solvent-and catalyst-free synthesis of 2-aryl (heteroaryl)-substituted benzothiazoles. Current Chemistry Letters. 2014;3(2):57-62.
32. Ikpa CB, Onoja SO, Okwaraji AO. Synthesis and antibacterial activities of benzothiazole derivatives of sulphonamides. Acta Chemica Malaysia. 2020 Dec 1;4(2):55-7.
33. Inamdar SM, More VK, Mandal SK. CuO nano-particles supported on silica, a new catalyst for facile synthesis of benzimidazoles, benzothiazoles and benzoxazoles. Tetrahedron Letters. 2013 Feb 6;54(6):579-83.
34. Alsahib SA, Baqer SR. Synthesis, identification of some new derivatives of 4-amino antipyrine bearing six and seven membered rings. InJournal of Physics: Conference Series 2021 Mar 1 (Vol. 1853, No. 1, p. 012010). IOP Publishing.
35. Gazi S, Patil SM. Synthesis and biological activities of some benzothiazole derivatives. Asian Journal of Research in Chemistry. 2010 Jun 28;3(2):421-7.
36. Yadav KK, Kumar A, Kumar A, Misra N, Brahmachari G. Structure, spectroscopic analyses (FT-IR and NMR), vibrational study, chemical reactivity and molecular docking study on 3, 3'-((4-(trifluoromethyl) phenyl) methylene) bis (2-hydroxynaphthalene-1, 4-dione), a promising anticancerous bis-lawsone derivative. Journal of Molecular Structure. 2018 Feb 15;1154:596-605.
37. Sharma PK, Amin A, Kumar M. A review: medicinally important nitrogen sulphur containing heterocycles. The Open Medicinal Chemistry Journal. 2020 Sep 14;14(1).

38. Al-Jibori SA, Waheed IF, Al-Samaraie AT. Synthesis and Characterization of Palladium (II) Complexes with 2-(2'-hydroxylphenyl) benzoxazole, 2-(2-hydroxyl phenyl) benzothiazole or the Mixed Ligands. Oriental Journal of Chemistry. 2012;28(1):257.
39. Nezhadali A, Rabani N. Competitive bulk liquid membrane transport of Co (II), Ni (II), Zn (II), Cd (II), Ag (I), Cu (II) and Mn (II), cations using 2, 2′-dithio (bis) benzothiazole as carrier. Chinese Chemical Letters. 2011 Jan 1;22(1):88-92.
40. Zehra S, Shavez Khan M, Ahmad I, Arjmand F. New tailored substituted benzothiazole Schiff base Cu (II)/Zn (II) antitumor drug entities: effect of substituents on DNA binding profile, antimicrobial and cytotoxic activity. Journal of Biomolecular Structure and Dynamics. 2019 May 3;37(7):1863-79.
41. Gorelsky SI, Lever AB. Electronic structure and spectra of ruthenium diimine complexes by density functional theory and INDO/S. Comparison of the two methods. Journal of Organometallic Chemistry. 2001 Oct 15;635(1-2):187-96.
42. Zhang S, Wang S, Wen Y, Jiao K. Synthesis and Crystal Structure of Hexakis (imidazole) nickel (II) O, O′-diphenyldithiophosphate [Ni (Im) 6](Ph2O2PS2) 2. Molecules. 2003 Dec 31;8(12):866-72.
43. Jamel HO, Adnan S, Mugheer TH, Jasim LS. Synthesis and Characterization of the Ligand (S, S'-Bis (Benzo [d] Oxazol-2-yl) 2, 2'-((Methylenebis (4, 1 Phenylene)) Bis (Azanediyl)) Diethanethioate (BMPAE) and it's Complexes with Some Transition Metals Ions. Journal of Global Technology. 2017;8(9):76-85.
44. Osowole AA, Wakil SM, Okediran EQ, Alao OK. Studies on Some Metal (II) Complexes of Mixed Ligands-Benzoic and N, N'-Dimethyldithiocarbamic Acids. Chem. J.. 2016;6:27-31.
45. Tolosa J, Ortiz CA. Caracterization of thin films by X'Pert-PRO PANalytical difractometer. MOMENTO-Revista de Física. 2014.
46. Stanjek H, Häusler WJ. Basics of X-ray Diffraction. Hyperfine interactions. 2004 Jun;154(1):107-19.
47. El-Sonbati AZ, Diab MA, El-Bindary AA, Mohamed GG, Morgan SM, Abou-Dobara MI, Nozha SG. Geometrical structures, thermal stability and antimicrobial activity of Schiff base supramolecular and its metal complexes. Journal of Molecular Liquids. 2016 Mar 1;215:423-42.
48. Serafińczuk J, Moszak K, Pawlaczyk Ł, Olszewski W, Pucicki D, Kudrawiec R, Hommel D. Determination of dislocation density in GaN/sapphire layers using XRD measurements carried out from the edge of the sample. Journal of Alloys and Compounds. 2020 Jun 5;825:153838.
49. Mahdi MA, Jasim LS, Mohamed MH. Synthesis and anticancer activity evaluation of novel ligand 2-[2-(5-Chloro carboxy phenyl) Azo] 1-Methyl Imidazole (1-Mecpai) with Some Metal Complexes. Systematic Reviews in Pharmacy. 2020 Dec 1;11(12):1979-87.
50. Qazi SJ, Rennie AR, Cockcroft JK, Vickers M. Use of wide-angle X-ray diffraction to measure shape and size of dispersed colloidal particles. Journal of Colloid and Interface Science. 2009 Oct 1;338(1):105-10.
51. Shukla M, Arya S. Determination of Chloride ion (Cl-) concentration in ganga river water by Mohr method at Kanpur, India. Green Chemistry & Technology Letters. 2018;4(1):6-8.
52. AL-Adilee KJ, Abass AK, Taher AM. Synthesis of some transition metal complexes with new heterocyclic thiazolyl azo dye and their uses as sensitizers in photo reactions. Journal of Molecular Structure. 2016 Mar 15;1108:378-97.
53. Kyhoiesh HA, Al-Adilee KJ. Synthesis, spectral characterization, antimicrobial evaluation studies and cytotoxic activity of some transition metal complexes with tridentate (N, N, O) donor azo dye ligand. Results in Chemistry. 2021 Jan 1;3:100245.
54. Rajivgandhi G, Saravanan K, Ramachandran G, Li JL, Yin L, Quero F, Alharbi NS, Kadaikunnan S, Khaled JM, Manoharan N, Li WJ. Enhanced anti-cancer activity of chitosan loaded Morinda citrifolia essential oil against A549 human lung cancer cells. International Journal of Biological Macromolecules. 2020 Dec 1;164:4010-21.
55. Yang J, Mu WW, Liu GY. Synthesis and evaluation of the anticancer activity of bischalcone analogs in human lung carcinoma (A549) cell line. European Journal of Pharmacology. 2020 Dec 5;888:173396.